

Multiplexed Spectral Signature Detection for Microfluidic Color-Coded Bioparticle Flow

Nien-Tsu Huang,[†] Steven C. Truxal,[†] Yi-Chung Tung,[†] Amy Y. Hsiao,[‡] Gary D. Luker,[§] Shuichi Takayama,[‡] and Katsuo Kurabayashi^{*,†,||}

Departments of Mechanical Engineering, Biomedical Engineering, Radiology and Microbiology and Immunology, and Electrical Engineering and Computer Science Engineering, University of Michigan, Ann Arbor, 48109, United States, and Research Center for Applied Sciences, Academia Sinica, Taipei, 11529, Taiwan

Here, we report a high-speed photospectral detection technique capable of discriminating subtle variations of spectral signature among fluorescently labeled cells and microspheres flowing in a microfluidic channel. The key component used in our study is a strain-tunable nanoimprinted grating microdevice coupled with a photomultiplier tube (PMT). The microdevice permits acquisition of the continuous spectral profiles of multiple fluorescent emission sources at 1 kHz. Optically connected to a microfluidic flow chamber via a multimode optical fiber, our multiwavelength detection platform allows for cytometric measurement of cell groups emitting nearly identical fluorescence signals with a maximum emission wavelength difference as small as 5 nm. The same platform also allows us to demonstrate microfluidic flow cytometry of four different microsphere types in a wavelength bandwidth as narrow as 40 nm at a high (>85%) confidence level. Our study shows that detection of fluorescent spectral signatures at high speed and high resolution can expand specificity of multicolor flow cytometry. The enhanced capability enables multiplexed analysis of color-coded bioparticles based on single-laser excitation and single-detector spectroscopy in a microfluidic setting. The fluorescence signal discrimination power achieved by the optofluidic technology holds great promise to enable quantification of cellular parameters with higher accuracy as well as enumeration of a larger number of cell types than conventional flow cytometric methods.

Fluorescently color-coded cells, biomolecules, and microspheres enable multiparameter detection in disease screening,¹ molecular imaging,² DNA sequencing,³ microarray applications,^{4,5}

cellular function studies,⁶ and multiplexed bead-based assays.⁷ The ability to identify multiple fluorescence emissions with high specificity is needed to gain sufficient multiplicity in biological analytical methods. Color decoding achieved by analyzing the detailed spectral characteristics of fluorophores can meet this demand, allowing fluorescence emissions with significant spectral overlap to be distinguished.^{6,8–10} However, detection of multiple spectral signatures generally reduces measurement speed and throughput due to a larger volume of required information and suffers from the added complexity and cost of optics as compared to techniques based on intensity measurements with discrete spectral bands. To address this issue, we recently developed a highly sensitive dynamic spectroscopy technique. This technique enables *in situ* detection of optical emission spectra by incorporating a high-speed strain tunable nanoimprinted grating microdevice.¹¹ With this technique, we demonstrated the ability to track the optical spectrum of time-varying multiwavelength signals with 500 μ s time resolution, 5 nm spectral resolution, and sensitivity for pW optical powers.¹² Eliminating the need for long-time signal integration, this technique enables more than 3 orders of magnitude faster spectral acquisition for such weak fluorescence emissions than commercial portable spectrometers incorporating a stationary reflective grating and a charge-coupled device (CCD) detector (e.g., Ocean Optics, USB 4000). The demonstrated spectral resolution is of the same order of magnitude as that of these portable spectrometers.

Suspension microsphere assays, where capture ligands are immobilized on color-coded microspheres, are currently the common antibody-based multiplexed protein immunoassay platforms together with planar microarray technology-based assays.¹³

- (3) O'Brien, K. M.; Wren, J.; Davé, V. K.; Bai, D.; Anderson, R. D.; Rayner, S.; Evans, G. A.; Dabiri, A. E.; Garne, H. R. *Rev. Sci. Instrum.* **1998**, *69*, 2141–2146.
- (4) Timlin, J. A. *Methods Enzymol.* **2006**, *411*, 79–98.
- (5) Neumann, N. F.; Galvez, F. *Biotechnol. Adv.* **2002**, *20*, 391–419.
- (6) Hiraoka, Y.; Shimizu, T.; Haraguchi, T. *Cell Struct. Funct.* **2002**, *27*, 367–374.
- (7) Nolan, J. P.; Sklar, L. A. *Trends Biotechnol.* **2002**, *20*, 9–12.
- (8) Dicker, D. T.; Lerner, J. M.; El-Deiry, W. S. *Cell Cycle* **2007**, *6*, 2563–2570.
- (9) Levenson, R. M.; Mansfield, J. R. *Cytometry, Part A* **2006**, *69*, 748–758.
- (10) Haraguchi, T.; Shimizu, T.; Koujin, T.; Hashiguchi, N.; Hiraoka, Y.; Shimizu, T. *Genes Cells* **2002**, *7*, 881–887.
- (11) Tung, Y.-C.; Kurabayashi, K. *Appl. Phys. Lett.* **2005**, *86*, 161113.
- (12) Truxal, S. C.; Tung, Y.-C.; Kurabayashi, K. *Appl. Phys. Lett.* **2008**, *92*, 051116.
- (13) Ellington, A. A.; Kullo, I. J.; Bailey, K. R.; Klee, G. G. *Clin. Chem.* **2010**, *56*, 186–193.

* To whom correspondence should be addressed. E-mail: katsuo@umich.edu.
† Department of Mechanical Engineering, University of Michigan.
‡ Department of Biomedical Engineering, University of Michigan.
§ Department of Radiology and Microbiology and Immunology, University of Michigan.

|| Department of Electrical Engineering and Computer Science Engineering, University of Michigan.

|| Academia Sinica.

- (1) Perfetto, S. P.; Chattopadhyay, P. K.; Roederer, M. *Nat. Rev. Immunol.* **2004**, *4*, 648–654.
- (2) George, T. C.; Fanning, S. L.; Fitzgerald-Bocarsly, P.; Medeiros, R. B.; Highfill, S.; Shimizu, Y.; Hall, B. E.; Frost, K.; Basjji, D.; Ortyn, W. E.; Morrissey, P. J.; Lynch, D. H. *J. Immunol. Methods* **2006**, *311*, 117–129.

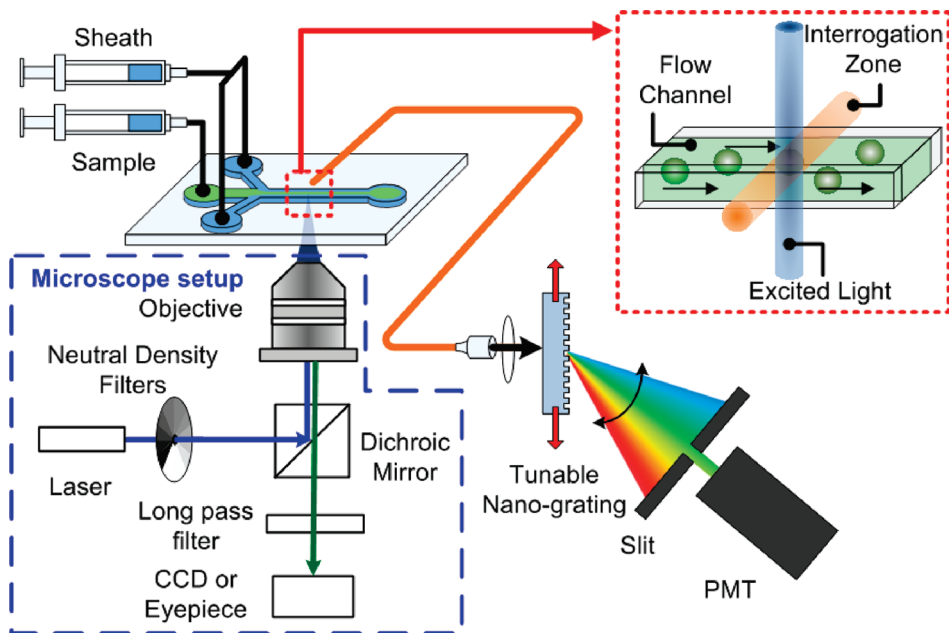


Figure 1. Schematic of the microfluidic multispectral flow cytometry (MMFC) setup. The system consists of a fluorescence microscope, microfluidic chamber, and spectroscopy units. The microfluidic flow chamber is placed on a microscope stage. Excitation laser light ($\lambda = 473$ nm) is focused on the interrogation zone of the microfluidic channel by the microscope objective lens. The spectroscopy unit is composed of a tunable nanograting microdevice, a single PMT, and a slit. Emission light from particles flowing in the microfluidic channel is collected at the probe of the embedded optical fiber (orange line). The collected light is collimated at the end of the optical fiber and dispersed after its transmission through the transparent grating microbridge of the microdevice. The grating diffracts the transmitting light and changes the diffraction angle with its grating pitch varied by the lateral movement of on-chip actuators (text and Figure S-1A, Supporting Information). The magnified image of the microfluidic channel shows the particle flows (red region). When the particles pass through the interrogation zone, they are optically excited and emit fluorescent signals fed to the embedded optical fiber. A data acquisition system (PCI-6111, National Instruments) and LabVIEW7.0 software (National Instruments) are used to capture the PMT signal and to apply an actuation voltage to the MEMS comb drives.

High-throughput analysis of microspheres is performed by fluorescence flow cytometry. In a fluorescence flow cytometry setting, fluorescently labeled particles are hydrodynamically injected into a capillary channel to form a single-profile flow, and their emission signals are excited by laser light and quantitatively characterized. Here, selective identification of multiple fluorescent molecular markers is also essential to discriminate diverse analyte species in the original sample mixture. However, a large hurdle against achieving high specificity and accuracy in multicolor flow cytometry arises when there are similarities and overlaps in the emission spectra of different dyes.¹⁴ For example, flow cytometers using as many as 11 fluorescent probe colors have been demonstrated to elucidate complex immune systems.¹⁵ However, these instruments require a large number of filters and detectors and only permit discrete ($\Delta\lambda = 40\text{--}90$ nm) spectral measurement, thus prohibiting color discrimination of fluorescent probes with only slight differences in wavelength characteristics. Applying our dynamic *in situ* spectroscopy technique to a flow cytometry setting provides an ideal opportunity for us to demonstrate the capabilities of our microdevice. This device enables the flow cytometry instrument to carry out continuous detection with significantly higher spectral resolution using a smaller, technically simpler optical design with a vastly reduced number of components.

In this paper, we integrate our strain-tunable nanoimprinted grating microdevice with a microfluidic flow chamber using simple fiber optics. The established system enables “microfluidic multi-

spectral flow cytometry” (MMFC), which is a flow cytometric measurement technique capable of quantitatively analyzing the spectral signatures of various particles at high speed in a microfluidic system. We demonstrate the system’s capability of differentiating spectrally similar emissions from GFP/Calcein-AM or GFP/YFP in living cells and four types of color-coded polystyrene microspheres flowing in microfluidic channels. We show that the spectral signature information obtained from the high speed (1 kHz) and spectral resolution (5 nm) of our device is the key to enabling flow cytometry with unprecedented multiplicity of up to four colors and specificity at a more than 85% confidence level for an optical band as narrow as 40 nm. Our technique enables the multiplexed flow cytometry with a simple optical system only consisting of a single excitation laser and a single detector. Compared to conventional methods, MMFC can differentiate more subtle parametric variances at high accuracy. Thus, we could add more analytical parameters in flow cytometry with multiple combinations of colors and/or spectral shape variations.

EXPERIMENTAL SECTION

Microfluidic Multispectral Flow Cytometry (MMFC) Setup.

The MMFC is constructed with three units: (1) a fluorescent microscope with an excitation laser ($\lambda = 473$ nm); (2) a microfluidic flow chamber; and (3) a spectral detection system consisting of a strain-tunable nanoimprinted grating microdevice and a single photomultiplier tube (PMT) with a slit (Figure 1 and Figure S-1, Supporting Information). The microfluidic channel is placed on the stage of the fluorescent microscope, which provides a

(14) Baumgarth, N.; Roederer, M. *J. Immunol. Methods* 2000, 243, 77–97.

(15) De Rosa, S. C.; Herzenberg, L. A.; Herzenberg, L. A.; Roederer, M. *Nat. Med.* 2001, 7, 245–248.

convenient platform for focusing light and aligning the microfluidic channel. The sample flow is hydrodynamically focused by two sheath flows of buffer solution. The resulting width of the focused sample flow is 30–50 μm . The use of a 60 \times objective (N.A. = 1.4) and an embedded optical fiber enables fluorescence excitation and detection with a highly focused interrogation zone. This fully eliminates light scattering from the edges of the channel, thereby significantly improving the signal-to-noise ratio of the measurement. The PMT provides high signal sensitivity and a fast acquisition rate. By adjusting the angular position of the PMT, we can set up the wavelength range to cover the detected emission spectra.

Microfabrication of the Nanoimprinted Grating Microdevice. To fabricate the strain-tunable nanoimprinted grating microdevice incorporated in the spectroscopy system, we use a fabrication method named the multilevel soft lithographic lift-off and grafting (ML-SLLOG).^{16,17} The fabrication process involves (i) construction of micrometer-to-millimeter scale silicon comb drives on a silicon-on-insulator (SOI) wafer, (ii) soft-lithographic replica molding and lift-off of a three-dimensional PDMS grating microbridge, and (iii) grafting and assembly of the PDMS microbridge onto the silicon comb drives, assisted by surface tension at an air–water interface. An actuator design with a series of 50 μm -thick silicon comb drives is employed as an extension of previous one developed by our group.¹⁷ The design of our previous device is modified to achieve a larger displacement of motion and a stronger actuation force for this study. The PDMS (Dow Corning Corporation; 10:1 base-curing agent ratio) microbridge has a surface feature of 350 grating lines with a nominal period of 700 nm and a height of 350 nm (text and Figure S-1A, Supporting Information). According to the Rayleigh criterion, the wavelength of interest and the number of grating lines determine the spectral resolution. The higher density and quality obtained for the new device design improve the resolving power of the grating. Oxygen plasma treatment for the surfaces of the PDMS grating microbridge bottom and the silicon comb drives is used to promote permanent bonding. Our previous study¹⁷ shows that the PDMS-silicon bonding is strong enough to sustain more than 100 million cycles of operation.

Construction of the Microfluidic Flow Cytometer. The optofluidic configuration for the microfluidic flow cytometer was originally proposed in our previous study.¹⁸ The microfluidic chamber is fabricated using PDMS soft lithography with a mold of patterned photoresist. The replicated PDMS structure is then bonded to a 200 μm thick glass slide that forms the bottom layer sealing the chamber. The flow channel cross-sectional area is 100 $\mu\text{m} \times 100 \mu\text{m}$. The optical fiber with a 100 μm diameter core and numerical aperture (N.A.) of 0.22 (F-MCB-T-3 SMA, Newport Corp.) is embedded perpendicular to the microfluidic channel to capture the emission signals from in-flow particles at high efficiency. The integrated fiber serves as an optical waveguide with small signal loss, thus leading to a high signal-to-noise ratio. The optical image is shown in the Supporting Information (Figure S-1B).

(16) Tung, Y.-C.; Kurabayashi, K. *J. Microelectromech. Syst.* **2005**, *14*, 558–566.

(17) Truxal, S. C.; Tung, Y.-C.; Kurabayashi, K. *J. Microelectromech. Syst.* **2008**, *17*, 393–401.

(18) Tung, Y.-C.; Zhang, M.; Lin, C.-T.; Kurabayashi, K.; Skerlos, S. J. *Sens. Actuators, B* **2004**, *98*, 356–367.

Sample Preparation. 293T cells are cultured in a Dulbecco's Modified Eagle Medium (Invitrogen, Carlsbad, CA, USA) with 10% fetal bovine serum, 1% glutamine, and 0.1% penicillin/streptomycin. Cells are transiently transfected with CXCR7 fused to GFP or the mcherry variant of YFP (CXCR7-GFP and CXCR7-YFP) as described previously.¹⁹ Two days after transfection, cells are mixed at CXCR7-GFP cell to CXCR7-YFP cell ratios of (1) 1:3, (2) 1:1, or (3) 3:1 as enumerated with a hemacytometer. Cells are resuspended in PBS at 2×10^6 cells/mL for the experiments.

HeyA8 and HeyA8-GFP ovarian cancer cell lines are cultured and maintained in complete media consisting of DMEM (11995, Gibco) supplemented with 10% (v/v) heat-inactivated fetal bovine serum (FBS, 10082, Gibco) and 1% (v/v) antibiotic–antimycotic solution (15240, Invitrogen). HeyA8-GFP cells were generated by lentiviral transduction with vector FUGW.²⁰ HeyA8 and HeyA8-GFP cells are routinely passaged at 70–90% confluence. All cultures are maintained in a humidified incubator at 37 °C, 5% CO₂, and 100% humidity. Live staining of HeyA8 cells was performed using the Calcein AM component from the LIVE/DEAD Viability/Cytotoxicity Kit for mammalian cells (L-3224, Invitrogen). Calcein AM diluted in PBS to a final concentration of 1 $\mu\text{g}/\text{mL}$ was added to HeyA8 cells and incubated for 30 min at 37 °C.

Four color polystyrene microspheres with a nominal diameter of 15 μm are used as suspension substrates in 10 mL of 0.15 M NaCl with 0.05% Tween 20 and 0.02% thimerosal. The suspensions (~0.2% solids) contain 1.0×10^6 microspheres per milliliter. In this experiment, each microsphere coded by one of green (F-21010), yellow-green (F-8844), yellow (F-21011), or orange (F-8841) fluorescent dyes (FluoSpheres, Invitrogen Co.). The peak excitation/emission spectra of these microsphere are 450/480 nm; yellow-green, 505/515 nm; yellow, 515/534 nm; and orange, 540/560 nm.

RESULTS AND DISCUSSION

Using the MMFC setup, we first demonstrate dynamic *in situ* spectral detection for particles in flow. Here, a solution of green colored polystyrene microspheres with PBS buffer is loaded into the sample syringe. Both the sample and sheath flow rates are set to be 5 $\mu\text{L}/\text{min}$. Data show 30 intensity peaks in a 1 s time window (Figure 2A), each coming from the emission of a green polystyrene microsphere passing. The time evolution of individual PMT signals in response to the actuation voltage signal of the mechanically tunable nanoimprinted grating microdevice is shown in the magnified time scale (Figure 2B). A single spectral sweep is completed as either the single stretching or contracting cycle of the grating takes place in 500 μs . The spectral acquisition speed is limited by the resonance frequency of the nanoimprinted grating microdevice (~3 kHz). In our experiment, we choose to operate the device at 1 kHz. This frequency is sufficiently lower than the resonance frequency and allows us to avoid causing any structural instability to the device. As a result, reliable and repeatable data acquisition is achieved. With the grating periodicity known for any actuation voltage level, the wavelength of the monochromatic

(19) Luker, K. E.; Gupta, M.; Steele, J. M.; Foerster, B. R.; Luker, G. D. *Neoplasia* **2009**, *11*, 1022–1035.

(20) Lois, C.; Hong, E. J.; Pease, S.; Brown, E. J.; Baltimore, D. *Science* **2002**, *295*, 868–872.

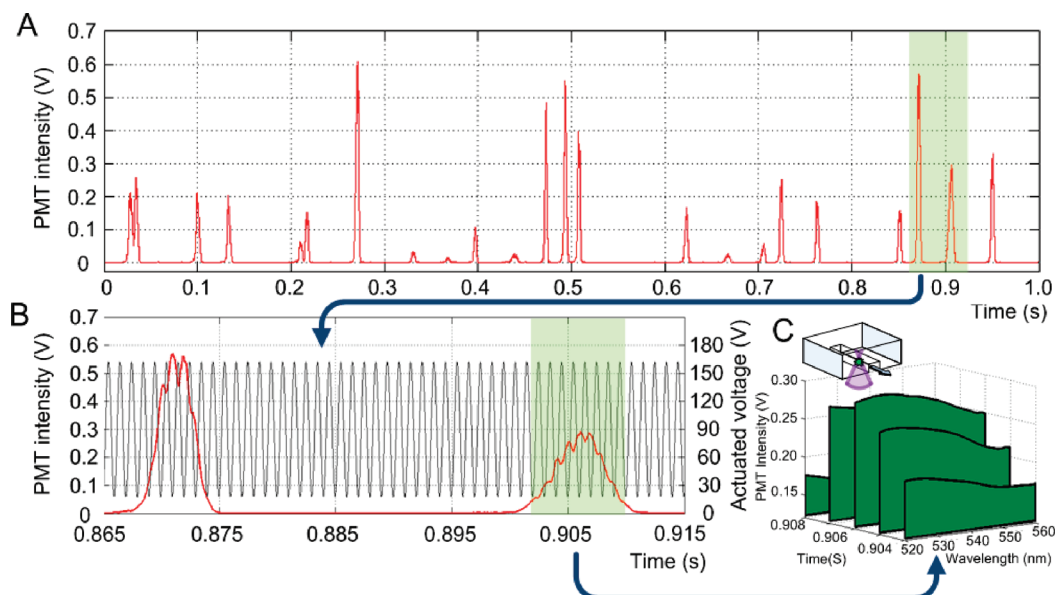


Figure 2. Time-domain data resulting from the dynamic in situ spectral detection of in-flow particles. (A) A time-domain plot showing PMT signals. The spectral signatures of more than 30 green colored polystyrene microspheres are detected in a 1 s time window using the MMFC setup. (B) A magnified plot of the PMT signals (red curve) superimposed with the corresponding actuation voltage signal applied to the MEMS comb drive actuators (black curve) in a 0.865–0.915 s interval. The MEMS actuation frequency is 1 kHz. A sinusoidal MEMS actuation voltage (140 V peak to peak with 20 V DC offset) is set at 1 kHz to perform high-speed spectral sweeping. The PMT signals are obtained at a 1 MHz acquisition rate. (C) A plot of the real-time spectral signals from a flowing single green colored polystyrene microsphere (the maximum emission at $\lambda = 523$ nm) that is constructed from 5-sweep spectral measurements within 5 ms. The PMT signal data are converted to the spectral plots based on a strain–voltage calibration curve and the grating equation.¹⁷ Here, the PMT intensity is given in terms of the output signal voltage.

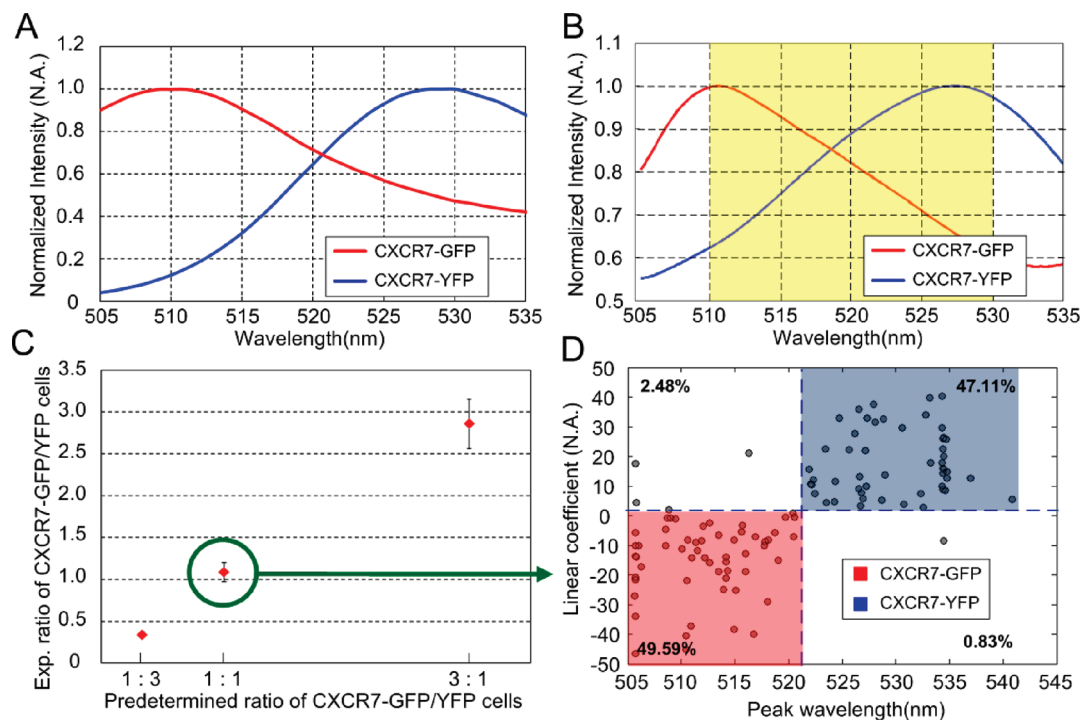


Figure 3. Discrimination of fluorescent proteins with similar spectra by MMFC. (A) Standard normalized emission spectrum of GFP and the mCitrine variant of YFP (19). (B) Normalized emission spectrum of GFP and YFP measured by MMFC setup. The linear coefficient of spectrum is resolved in a 510–530 nm wavelength range (yellow region). (C) Comparison of the predetermined and experimentally measured population ratios for mixtures of suspended CXCR7-GFP and CXCR7-YFP cells. Samples of three CXCR7-GFP/YFP cell fractions, (i) 1:3, (ii) 1:1, and (iii) 3:1, are prepared by hemocytometry prior to the MMFC measurements. The experimental data with $N = 125, 199$, and 387 for samples (i), (ii), and (iii), respectively, are obtained by a 30 s measurement. (D) The 2D plot maps the peak wavelength and linear coefficient taken for a particular 1:1 cell control mixture (green circle in (C)). By carefully selecting the cutoff boundary, we can sort out 49.59% CXCR7-GFP and 47.11% CXCR7-YFP cells of total cell population flowing by in 30 s. This experiment yields the expected values well, thus validating the accuracy of the MMFC technique for cells coded with spectrally similar fluorescent proteins.

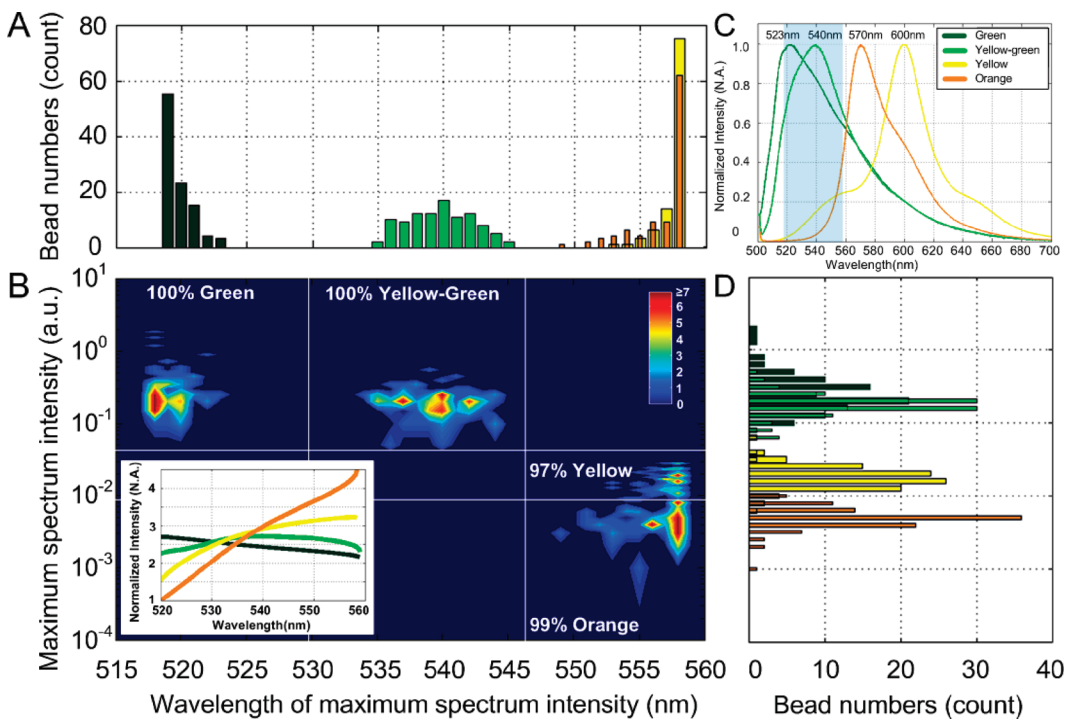


Figure 4. Four color discrimination of polystyrene microspheres in a 518–558 nm wavelength (λ) range (shadowed region in (C)) by MMFC. Each particle flows through the microfluidic channel and its spectral signature is captured from the PMT signal. The polystyrene microspheres are named according to their emission colors: (i) green, (ii) yellow-green, (iii) yellow, and (iv) orange. Each sample group consists of $N = 100$ data points. (A) A univariate histogram of the wavelength of maximum spectrum intensity at $\lambda = 518$ – 558 nm. (B) A population density contour plot for the maximum spectrum intensity and the wavelength of maximum spectrum intensity at $\lambda = 518$ – 558 nm. The percentage values represent the confidence levels of data discrimination with the dividing lines. The subfigure shows normalized fluorescence emission spectra for the polystyrene microspheres. (C) Spectral data of the microspheres measured by a commercial spectrometer (Ocean Optics, USB4000). (D) A univariate histogram of the maximum spectrum intensity at $\lambda = 518$ – 558 nm. This multiparameter spectral analysis allows for differentiating the four-color spectral signatures with significant overlaps in the 40 nm wavelength bandwidth.

light incident at the angle of the PMT is calculated using the grating equation, which allows us to construct spectrum plots.^{12,21} In this measurement, nearly five spectral sweeps within a 5 ms time window can be performed for each passage of a single microsphere in front of the optical fiber probe (Figure 2C). Using a quadratic curve fitting method (text and Figure S-2, Supporting Information), we can obtain the linear coefficient of this continuous spectrum profile as another characteristic parameter (text, Supporting Information), which provides additional information to help discriminate different sample groups.

With the spectral acquisition process established for our optofluidic system, we further demonstrate the ability to discriminate two spectrally similar fluorescent proteins by MMFC. The cell groups consist of human embryonic kidney 293T cells transfected with CXCR7 fused to green fluorescent protein (GFP) or the mCitrine variant of yellow fluorescent protein (YFP). The standard emission spectra of GFP and YFP have a significant spectral overlap (Figure 3A).²² From the MMFC setup, we can reconstruct these two similar spectra, and the linear coefficient of each spectrum can be resolved in a 510–530 nm wavelength range. We prepare samples with three known population fractions of CXCR7-GFP and CXCR7-YFP cells: (i) 1:3; (ii) 1:1; and (iii) 3:1. Samples flow into the microfluidic channel for MMFC measurements, and spectral data for individual cells are obtained for 30 s.

We analyze the characteristics of the continuous spectral plot for each cell flowing through the interrogation zone that are quantified by peak wavelength (i.e., the wavelength value of maximum emission), peak intensity (i.e., the intensity value of maximum emission), and linear coefficient (text and Figure S-2, Supporting Information). We count the numbers of cells belonging to the two color groups from the spectral characteristics and plot their ratio for each sample (Figure 3C). Here, we take 520 nm and 0 as the cutoff values for the peak wavelength and the linear coefficient, respectively, which are reasonable values judged from the spectra of GFP and YFP (Figure 3A,B). For example, the linear coefficient-versus-peak wavelength plot taken for the 1:1 sample shows two statistically distinct groups with a population ratio of nearly 1 (49.59% CXCR7-GFP and 47.11% CXCR7-YFP cells of total cell population; Figure 3D). Our data show good agreement between the experimentally measured and predetermined CXCR7-GFP/YFP cell population fractions for all of the samples (Figure 3C,D). This validates the numeration accuracy of the MMFC technique proposed here.

Subsequently, we perform dynamic *in situ* spectral detection for four types of in-flow polystyrene microspheres (15 μm in diameter) with different colors by MMFC. We adjust the tunable grating strain ratio and the PMT angle to achieve a 518–558 nm wavelength tuning range, where these microspheres exhibit notable spectral overlaps (Figure 4C). We find that the microsphere flow can maintain good stability at a higher flow rate. Therefore, the sample flow rate is increased to 10 $\mu\text{L}/\text{min}$ to

(21) Truxal, S. C.; Kurabayashi, K.; Tung, Y.-C. *Int. J. Optomechatronics* 2008, 2, 75–87.

(22) Shaner, N. C.; Steinbach, P. A.; Tsien, R. Y. *Nature* 2005, 2, 905–909.

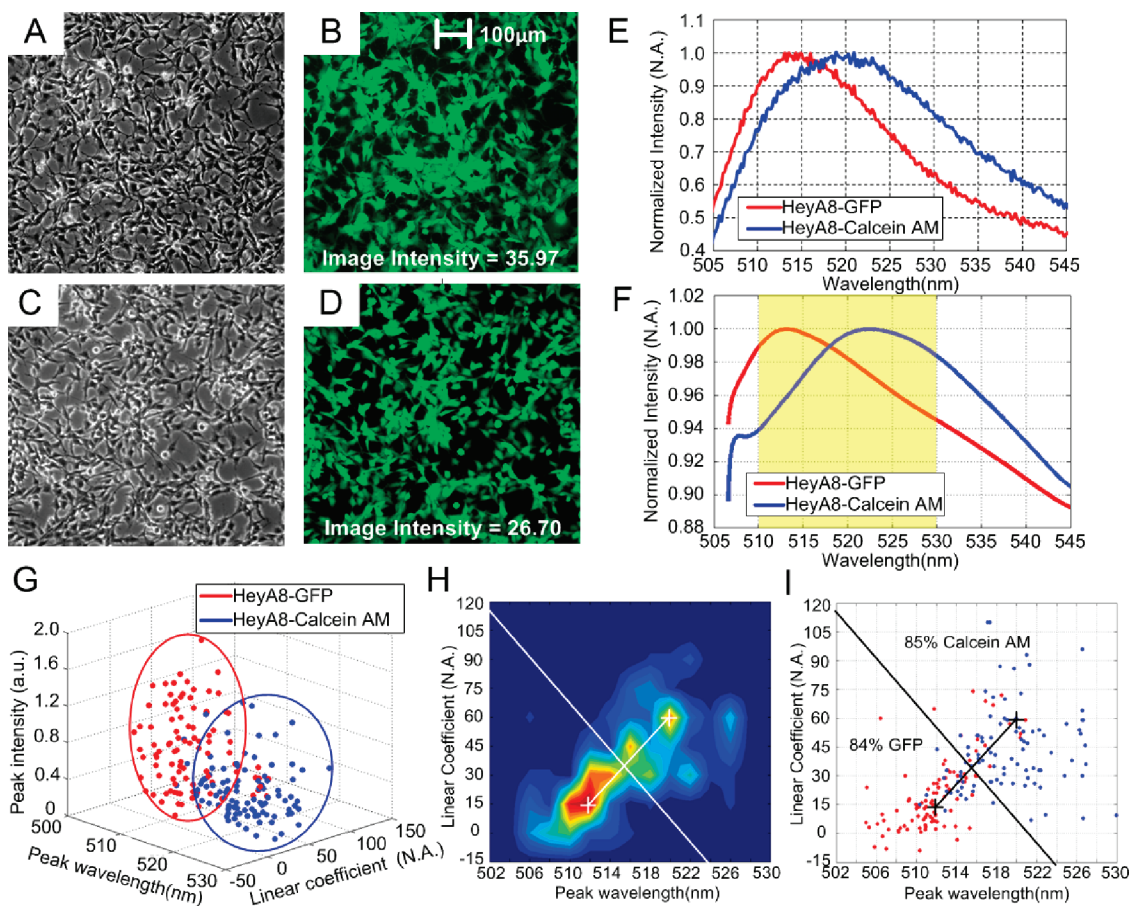


Figure 5. MMFC distinguishes fluorophores with nearly identical emission spectra in living cells. (A–D) 10 \times microscopy images of HeyA8-GFP cells in (A) the brightfield view and (B) the fluorescent imaging mode. 10 \times microscopy images of HeyA8-Calcein AM cells in (C) the brightfield view and (D) the fluorescent imaging mode. The fluorescent images are taken in the FITC filter band. The numbers in (B) and (D) represent the average fluorescence image intensity in the field of view. Because of the similar colors and fluorescence image intensity values, it is difficult to visually differentiate these two cell groups from the fluorescent images. Normalized fluorescence emission spectra of HeyA8-GFP and HeyA8-Calcein AM cells measured by (E) a commercial spectrometer (Ocean Optics, USB4000) and (F) MMFC setup. (G) Three-dimensional (3D) plot of the peak wavelength, peak intensity, and linear coefficient of the spectral signatures for both HeyA8-GFP and HeyA8-Calcein AM cells ($N = 181$). (H) Two-dimensional contour plot of peak wavelength vs linear coefficient obtained from the projection of (G). All the presented values of the linear coefficient are extracted by curve fitting to MMFC spectral plots in the $\lambda = 510\text{--}530$ nm wavelength range, i.e., the yellow region in (F). The perpendicular bisector of the line connecting the two population peaks is taken as the dividing line between the two regions. (I) The ratio of the GFP-labeled and Calcein AM-labeled cells whose data points fall in the GFP and Calcein AM regions are calculated on the basis of the cell distribution plot of peak wavelength vs linear coefficient, obtained from the projection of (G).

achieve higher throughput. From the continuous spectrum measurement, we can map the maximum intensity and wavelength of maximum intensity of each microsphere color type in the 518–558 nm wavelength range (Figure 4B). The histograms (Figure 4A,D) show the particle population distributions for each of these spectral parameters. Using the combination of the two parameters, the four fluorescent color bands of the polystyrene microspheres can be discriminated even in such a narrow wavelength bandwidth as 40 nm. Here, we prove that information from the continuous spectral plots provides high multiplicity for MMFC even if the wavelength bandwidth employed for the measurement is limited. It should be noted that the use of the particles coded by spectrally similar colors enables our system to carry out high-speed, multiplexed detection with a single excitation source and a single photodetector. This represents a capability unique to MMFC that has not been demonstrated with conventional flow cytometry settings.

We finally repeat the measurement at the sample flow rate of 5 $\mu\text{L}/\text{min}$ for two types of color-coded cells whose emission

spectra have very similar intensities and profiles. Here, we employ ovarian surface epithelial tumor cell lines, HeyA8, stably transduced with GFP and stained with Calcein AM (Figure 5A–D). The peak wavelengths of the HeyA8-GFP and HeyA8-Calcein AM emission spectra are 514 and 520 nm, respectively, which are measured by a commercial spectrometer (Figure 5E) and MMFC (Figure 5F). Because of their similar fluorescence intensities, i.e., spectrum intensities integrated over the wavelength band of the emission filter (text, Supporting Information), and spectral shapes, these fluorescent labels cannot be distinguished by conventional fluorescent microscopy or flow cytometry. Data obtained by a commercial flow cytometer show the inability to differentiate these two cell groups from their intensities measured by a conventional method (text and Figure S-3, Supporting Information). In contrast, with the combinations of the three characteristic parameters (e.g., peak wavelength, peak intensity, and linear coefficient) of the continuous spectral profiles, the cell groups can be clearly segregated in the three-dimensional (3D) cell population distribu-

tion space (Figure 5G). The mean value and standard deviation of HeyA8-GFP and HeyA8-Calcein AM cell groups for the three parameters are tabulated (Table S-1, Supporting Information). However, because the emissions of HeyA8-GFP and HeyA8-Calcein AM strongly depend on the expression level of GFP, the degree of Calcein AM staining strength, and the total number of alive cell population, the “peak intensity” may not be an intrinsic signature indicative to differentiate these two cell groups and will be, therefore, eliminated in our analysis later.

To quantitatively assess our system’s discrimination power for these two cell groups, we construct a two-dimensional (2D) cell population contour plot of peak wavelength vs linear coefficient (Figure 5H) from the 3D cell population distribution plot (Figure 5G). We first set 10–15 gridlines for each parameter in 2D cell distribution plots and, then, count the number of data points that fall in each mesh area. The value of this number is represented by the color of the mesh area. With this information, two regions with a GFP or Calcein AM population density peak are determined for each 2D contour plot. A perpendicular bisector of the line connecting the two population peaks is taken as the dividing line between the two regions. We then calculate the fractions of the GFP-labeled and Calcein AM-labeled cells whose data points fall in the GFP and Calcein AM regions for the cell distribution plots (Figure 5I). Each region includes nearly 85% of the total population of the particular cell group. The data points of the remaining 15% population that fall in the region of the other cell group represent false positives of the measurements.

The microfluidic platform described here represents a unique class of optofluidic system incorporating a MEMS-based tunable nanoimprinted grating microdevice, a single excitation laser, and a single PMT detector. The system enables us to demonstrate a technique named MMFC (microfluidic flow cytometry), capable of in situ continuous spectral profile detection for bioparticles flowing in a microfluidic channel with high specificity and high speed. Integrating our optofluidic system with other microfluidic components, we could develop a lab-on-a-chip system that enables multiplexed signal detection together with sample preparation/loading, agent mixing/reaction, cell culture, or programmable chemical stimulation on a single chip. Furthermore, systems

identical with ours could be integrated with an array of microfluidic channels to perform massively parallel cell analysis with higher throughput and multiplicity on a single chip. The use of microspheres as platforms for surface binding assays and analyses in microfluidic channels results in large surface-to-volume ratios, leading to the capacity to bind greater analyte molecules in a small volume.^{23–26} Therefore, microsphere-based MMFC promises high assay sensitivity.

Of particular note is that our study demonstrates in situ detection and discrimination of in-flow emission sources with only 5 nm peak-to-peak spectral difference and a significant intensity overlap at a confidence level as high as 85%. This capability is unique to our system and cannot be achieved by the optics of conventional flow cytometers, which only detect emission intensities with discrete wavelength bands (text and Figure S-3, Supporting Information). Our dynamic in situ spectroscopy technique has the potential to allow highly accurate quantification of protein binding, intracellular Ca²⁺ concentration, pH, and temperature in a flow cytometry setting based on subtle variations in the emission spectral profiles of probe fluorophores as well as from their intensity variations.^{27–29} Particularly for fluorescent proteins, our system could substantially improve the ability to discriminate among cell populations with protein combinations, such as CFP/GFP and GFP/YFP that cannot be separated by standard flow cytometry. This will, for example, allow researchers to combine and identify more cell types in genetically engineered mice. Our system could also provide new means to analyze structural and functional heterogeneities of cells to obtain information useful for disease diagnosis/prediction and drug discovery in microfluidic environments.

ACKNOWLEDGMENT

This work is supported by NSF (Grant EECS-061237), NIH (Grants R01 CA136553, R01 CA136829, R01 CA142750, P50 CA93990), Microfluidics in Biomedical Sciences Training Program from NIH (NIH/NIBIB T32 EB005582), the University of Michigan Horace H. Rackham Predoctoral Fellowship to A.Y.H., the University of Michigan Mechanical Engineering Graduate Fellowship to N.T.H., the DHS Graduate Fellowship to S.C.T.

SUPPORTING INFORMATION AVAILABLE

Additional information as noted in text. This material is available free of charge via the Internet at <http://pubs.acs.org>.

Received for review August 25, 2010. Accepted October 14, 2010.

AC102240G

- (23) Kellar, K. L.; Iannone, M. A. *Exp. Hematol.* **2002**, *30*, 1227–1237.
- (24) Verpoorte, E. *Lab Chip* **2003**, *3*, 60–68.
- (25) Alivisatos, P. *Nat. Biotechnol.* **2004**, *22*, 47–52.
- (26) Kellar, K. L.; Oliver, K. G. *Methods Cell. Biol.* **2004**, *75*, 409–429.
- (27) Zhu, B.; Jia, H.; Zhang, X.; Chen, Y.; Liu, H.; Tan, W. *Anal. Bioanal. Chem.* **2010**, *397*, 1245–1250.
- (28) Palmgren, M. *Anal. Biochem.* **1990**, *92*, 316–321.
- (29) Krasnowska, E. K.; Gratton, E.; Parasassi, T. *Biophys. J.* **1998**, *74*, 1984–1993.